

# Energy-Efficient Wake-Up Signalling for Machine-Type Devices Based on Traffic-Aware Long-Short Term Memory Prediction

David E. Ruíz-Guirola, Carlos A. Rodríguez-López, Samuel Montejó-Sánchez, *Senior Member, IEEE*, Richard Demo Souza, *Senior Member, IEEE*, Onel L. A. López, *Member, IEEE*, and Hirley Alves, *Member, IEEE*

**Abstract**—Reducing energy consumption is a pressing issue in low-power machine-type communication (MTC) networks. In this regard, the Wake-up Signal (WuS) technology, which aims to minimize the energy consumed by the radio interface of the machine-type devices (MTDs), stands as a promising solution. However, state-of-the-art WuS mechanisms use static operational parameters, so they cannot efficiently adapt to the system dynamics. To overcome this, we design a simple but efficient neural network to predict MTC traffic patterns and configure WuS accordingly. Our proposed forecasting WuS (FWuS) leverages an accurate long-short term memory (LSTM)-based traffic prediction that allows extending the sleep time of MTDs by avoiding frequent page monitoring occasions in idle state. Simulation results show the effectiveness of our approach. The traffic prediction errors are shown to be below 4%, being false alarm and miss-detection probabilities respectively below 8.8% and 1.3%. In terms of energy consumption reduction, FWuS can outperform the best benchmark mechanism in up to 32%. Finally, we certify the ability of FWuS to dynamically adapt to traffic density changes, promoting low-power MTC scalability.

**Index Terms**—Energy efficiency, machine-type communication, neural network, traffic prediction, wake-up signal.

## I. INTRODUCTION

Future cellular networks need to support and drive a large variety of existing, emerging, and even unforeseen, Internet of Things (IoT) use cases [1]–[3]. Indeed, machine-type communication (MTC) is an essential component of the fifth generation (5G) of wireless networks as it enables machine-type devices (MTDs) to communicate and interact with each other without human interventions [4]. Applications include mission critical services, intelligent transportation systems,

fleet management, smart grid, industrial automation, real-time monitoring/control, and remote medical systems [5]–[10]. Consequently, the number of MTDs is explosively growing, and billions of MTDs, such as sensors, actuators, and meters, are predicted to be operational in the coming years.

Energy efficiency is a key design requirement for IoT networks composed of MTDs that must operate for several years without battery recharging or replacement [11], [12]. Most of these MTDs have limited energy resources due to their small size, low cost and/or hard-to-reach locations [13]–[15], which poses unprecedented challenges on the radio access network [16]. A fundamental approach lies in bringing the complexity of IoT devices down by decreasing the computation capability, using low-order modulations, and introducing deep sleep modes [17]. Indeed, idle channel monitoring is one of the major energy consumption sources at the MTDs, particularly in networks with low traffic [18]. In this regard, the 3rd generation partnership project (3GPP) introduced wake up radios (WuRs) in its Release 15 [19] to prolong the lifetime of battery-powered devices. For both, long term evolution for MTC (LTE-M) and narrow-band IoT (NB-IoT), device power consumption in idle mode is reduced by exploiting a wake-up signal (WuS). Similarly, IEEE 802.11 introduced WuS in the IEEE 802.11ba amendment [20], [21].

For many NB-IoT use cases envisioned by 3GPP, communication is infrequent over long periods of time [22], and therefore the standard includes Discontinuous or Extended Discontinuous Receive (DRX or eDRX) mode in idle operation [22]. During DRX/eDRX, the device waits for the reception of regular paging events (occasions) to decide whether to switch to active mode. Such paging events are preceded by the transmission of a narrowband WuS to allow the device to remain in a low power state by default, and only wake-up to decode a paging event if the WuS is identified [23].

WuS is transmitted within a configurable time before the device is paged, page occasion (PO), maximizing the sleep time [18], [24], [25]. As MTDs avoid frequent wake-ups from listening to paging information not intended for them, the power consumption in idle mode reduces. Thus, a low-complexity wake-up receiver is an essential requirement [3]. A paradigm shift from the traditional duty cycling (DC) medium access control (MAC) operation to on-demand WuR operation is envisaged due to the latter's energy efficiency superiority [26]. It has been shown in [27] that a WuR's average power consumption is around 1000 times lower than that of

David E. Ruíz-Guirola, Onel L. A. López and Hirley Alves are with the Centre for Wireless Communications University of Oulu, Finland. {David.RuizGuirola, Onel.AlcarazLopez, Hirley.Alves@oulu.fi} Carlos A. Rodríguez-López is with the Department of Electronics and Telecommunications, Universidad Central “Marta Abreu” de Las Villas, Santa Clara, Cuba. {crodriguez@uclv.edu.cu} Samuel Montejó-Sánchez is with the Programa Institucional de Fomento a la Investigación, Desarrollo e Innovación, Universidad Tecnológica Metropolitana, Santiago, Chile. {smontej@utem.cl} Richard Demo Souza is with the Federal University of Santa Catarina, Florianópolis, SC, Brazil. {richard.demo@ufsc.br}

This work has been partially supported in Chile by ANID FONDECYT Iniciación No. 11200659, FONDECYT-EM-180180, and Collaborative Research Activities between PIDi/UTEM and FIE/UCLV, in Brazil by CNPq (402378/2021-0, 305021/2021-4), Print CAPES-UFSC “Automation 4.0”, and RNP/MCTIC (Grant 01245.010604/2020-14) 6G Mobile Communications Systems, and in Finland by 6Genesis Flagship (Grant no. 318927) and Tekniikan Edistämissäätiön.

TABLE I  
BRIEF SUMMARY ON BENCHMARKS AND OUR PROPOSAL

Ref.	Features
DRX [30]	Standard DRX mechanism with optimized parameters, Poisson traffic model, traffic analysis, target mean delay
WuS [37]	Standard WuS, predefined time interval between low-power states with beacon seeker (WRx-On), Poisson traffic model, traffic analysis, target mean delay
FWuS	Low-power MTC traffic model using PPPs, AI-based traffic analysis, dynamic forecasting model to optimize WuS parameters, adjustable time interval between WRx-On states, target mean delay

the main radio. Furthermore, the implemented WuR in [28] achieves around 70 times longer lifetime than DC protocols (with 1% duty cycling) under light traffic load. With such potential energy savings, WuR appears as a promising technique for achieving a lifespan beyond 10 years, which is the targeted lifetime for NB-IoT and 5G IoT devices. Moreover, WuR enables instantaneous response to on-demand IoT data transmissions, resulting in much shorter latency [26].

Improving the efficiency of the standardized DRX mechanism for MTC has been the focus of much attention, e.g., [11], [29]–[32]. Authors in [29], [30] discuss the tuning of a given set of DRX parameters in LTE/LTE-A and analyze the impact on energy-efficiency, while an improvement to DRX based on the inactivity timer management is provided in [31]. Authors in [32] propose a DRX mechanism that exploits the radio resource control connection release and re-establishment to save significant energy in MTDs, while an artificial intelligence (AI)-based adaptive DRX is devised in [11]. However, since the DRX mechanism is not specifically designed for MTDs, more suitable mechanisms are required [33].

Meanwhile, MTDs operating with WuR are considered in [18], [34]–[37]. Specifically, authors in [34] consider low-complexity WuS to improve energy-efficiency while MTC re-synchronization is carried out. The benefits of using passive WuR in wireless energy harvesting networks are highlighted in [35], whereas efforts to improve WuS in interference-free OFDM based systems are made in [18]. In all cases, WuS mechanisms use static operational parameters, which in [36], [37] are determined by the base station (BS) at the beginning of the session. Remarkably, AI-based mechanisms for efficiently tuning WuS parameters in low-power MTC networks, although naturally appealing, remain unexplored. Therefore, we consider there is vast potential for further reducing energy consumption by incorporating intelligence into WuS.

Herein, we aim at designing an efficient AI-enabled WuS mechanism. The main contributions of this paper are outlined next. First, we model the position of MTDs and event epicenters as distinct and independent Poisson point processes (PPPs), and define a function to model the influence of events on MTC traffic. It is noteworthy that the model is able to characterize the different traffic patterns described in the literature, e.g., [38]–[40]. We leverage a simple neural network (NN) to predict MTC traffic patterns and configure

TABLE II  
TABLE OF ACRONYMS

Symbol	Description
A	Active state
DRX	Discontinuous reception
FWuS	Forecasting WuS
I	Idle state
LSTM	Long short-term memory
MTC	Machine-type communication
MTD	Machine-type device
NB-IoT	Narrow-band internet of things
PDWCH	Physical downlink wake-up channel
PO	Page occasion
PPP	Poisson point process
RFI	Radio frequency interface
RMSE	Root mean square error
RNN	Recurrent neural network
TTI	Transmission time interval
WuR	Wake-up radio
WRx-On	Low-power state with beacon seeker
WuS	Wake-up signal

WuS accordingly. We refer to such mechanism as forecasting WuS (FWuS). Then, we use FWuS to optimize the wake-up parameters of the MTDs. In addition, the mean delay and power consumption performance are quantified for a set of wake-up parameters. Finally, numerical results evince the superiority of our proposed method with respect to WuR [37] and DRX [30] based reference mechanisms. Table I summarizes the main features of the proposed solution and the benchmarks. To the best of our knowledge, optimizing WuS in this type of scenario has not been proposed before. Our work takes on significant relevance when considering the ever increasing number of connected MTDs, the urge for reducing their energy consumption down to actual operation requirements, and societal and economic goals regarding sustainable.

The rest of this paper is organized as follows. Section II describes the system model, while Section III overviews WuS technology and describes the traffic model. Section IV formulates the problem and introduces the proposed scheme. Section V describes the framework for evaluating the system performance. Numerical results are illustrated in Section VI, and conclusions are drawn in Sections VII. Tables II and III list respectively acronyms and symbols used throughout this paper. For simplicity, we have omitted the well-known acronyms.

## II. SYSTEM MODEL

We consider the coverage area of a single BS, where multiple coordinators [41] are deployed to serve as gateways of short-range MTDs, as depicted in Fig. 1. This allows saving energy at the MTDs, which otherwise would need more power to communicate with the BS, and serves as a solution to those MTDs that cannot directly contact the BS due to the use of short range communication technologies [42]. The MTDs are equipped with a WuR module to save energy by allowing the radio frequency interface (RFI) to monitor the medium at regular intervals looking for triggering signals. Each coordinator controls all the information exchange within its cell, deciding whether to send a WuS that allows the MTD to exchange information.

Note that in some applications the coordinator is in charge of granting/scheduling access to MTDs that have requested it

TABLE III  
LIST OF SYMBOLS

Symbol	Description
$d$	Distance between the place of occurrence of an event and the position of a sensor
$D$	Packet delay
$\bar{D}$	Mean packet delay
$p(d)$	Distance function
$g_i$	Predictions of inter-arrival time (expected values)
$g_{oi}$	Observed inter-arrival time (known results)
$P_A$	Probability that a device goes to active mode
$p_f$	False detection probability
$p_i$	Probability of being in $S_i$
$P_{ij}$	Transition probability from a state $S_i$ to $S_j$ , $P(S_j S_i)$
$p_{md}$	Miss-detection probability
$PW$	Mean power consumption
$PW_i$	Power consumption in $S_i$
$PW_b$	Power consumption of a benchmark scheme
$q$	Geometrical distribution parameter
$R(k, s)$	Traffic rate in a time slot $k$ and state $s \in I, A$
$S_i$	WuS state; $i = (1, 2, 3, 4)$
$t_{mac}$	Delay due to the MAC protocol
$t_{on}$	On time
$t_{pd}$	Power down time
$t_{sleep}$	Forecasted sleep time
$t_u$	Start up time
$t_1$	WRx-On time
$t_2$	Active-decoding time
$t_3$	Inactivity time
$t_4$	Sleep time
$\eta$	Relative power saving
$\eta_{max}$	Maximum relative power saving
$\eta_{min}$	Minimum relative power saving
$\lambda_E$	Event density
$\lambda_M$	MTDs' density
$\Phi_E$	PPP of event epicenters
$\Phi_M$	PPP of MTDs deployment

[15], [38], [43]. However, in some others, the MTDs need to be attentive to the coordinator [37], [44], which may inform the MTD of event anticipation or about an event that was not sensor-detected. In this way, MTDs need to be checking the physical downlink wake-up channel (PDWCH) regularly because, even when their sensors have not been activated by an event, the coordinator still may request information from them, or for anticipating future activation for smooth applications like target tracking. An appealing approach may be that in which a coordinator activates specific MTDs based on AI-enabled forecasting mechanisms. Such mechanisms can be deployed at the coordinator side to keep the MTDs simple and energy-efficient. Moreover, the coordinators can control the medium access, avoid collisions, and consequently reduce the energy consumed by the MTDs when they are not scheduled and would be performing idle listening [45], [46].

For the sake of contextualization, consider the following potential scenarios: i) target tracking, and ii) visitors of a historic arena. In the first case, MTDs that detect an event may trigger the surrounding nodes, and a set of MTDs activated by the coordinator may track/localize the target. Activating only the sensors close to the path followed by the target is a reasonable approach. The awakened group of MTDs may localize the target accurately. In the second scenario, the objective of the MTC network is to detect the visitors who are trying to enter forbidden areas. During the open hours of the museum, the rate of these events may be larger than during

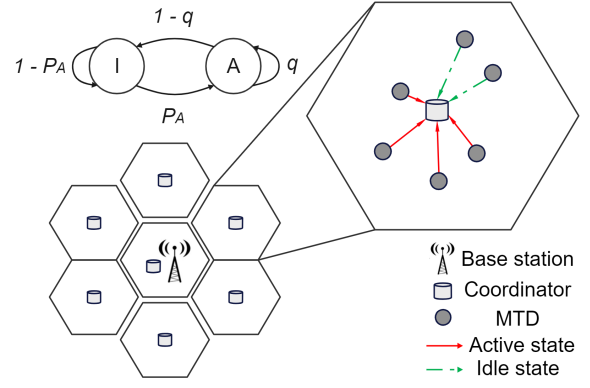


Fig. 1. Illustration of an MTC network where the coverage area of the BS is split in several smaller areas<sup>1</sup> in which a coordinator controls and collects information from the MTDs. Traffic exchanged between MTDs and the coordinator is modeled as a two-state complete Markov chain.

the night shifts. Daytime operation of the network can be based on periodic WuS scheduling, whereas nighttime operation can follow a more suitable wake-up approach.

#### A. MTDs Deployment and Event Sensing

Consider a single coordinator and let the MTDs be deployed randomly and independently in its coverage area. We resort to homogeneous PPPs to model the position of devices and event epicenters [47]. Note that PPP has been the most popular spatial model for various types of wireless networks [48], [49] because of salient features such as the independence between points and the simple form of the probability generating functional [50]. The PPPs of the MTDs positions and event trigger epicenters in the Euclidean plane are denoted respectively by  $\Phi_M$  and  $\Phi_E$ . These processes are assumed to be independent and to have density  $\lambda_M$  and  $\lambda_E$ , respectively.

Let  $p(d)$  denote the probability that a certain MTD senses an event with epicenter at a distance  $d$  in the Euclidean plane  $\mathbb{R}^2$ . Then, we have  $p(d) : [0, \infty) \rightarrow [0, 1]$ , where  $p(d)$  is typically non-increasing to represent a decaying influence of events as the distance  $d$  increases. Fig. 2 depicts an instantaneous realization of the MTC network and event epicenters.

#### B. MTD State Modeling

Each MTD has sensors that trigger an interrupt if they detect an event (e.g., a peak in energy consumption or a relevant variation in energy consumption). Upon detecting an event, the MTD connects the necessary parts to process this signal, which had been turned OFF to save energy [51]. The information is stored in the MTD awaiting an RFI activation signal from the coordinator. The MTD measures and processes, but does not transmit until indicated by the coordinator.

Each MTD can be in one of two states:

- 1) idle ( $I$ ): the MTD wakes up (ON) the RFI at regular intervals, while it waits a WuS from the coordinator.

<sup>1</sup>This paper focuses only on intra-cell communication. Note that cells do not have to be precisely hexagonal or the same size, since the MTDs deployment density ( $\text{MTDs}/m^2$ ) depends on the area and not on the shape of the region of interest. We adopted the current representation for aesthetic reasons and in analogy to the classical literature on mobile communications.

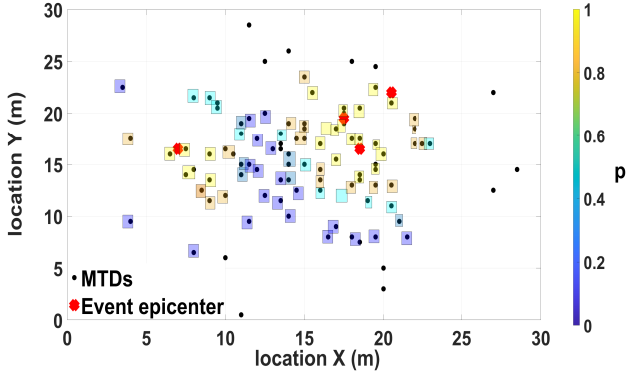


Fig. 2. Illustration of the influence of events on the surrounding MTDs. Colored squares are related to the event activation probability in the colorbar (right). The absence of a square means zero activation probability.

The MTD may experience a sensor-detected interrupt, however, that information is stored and the MTD remains in state *I* until receiving a WuS. The MTD saves considerable energy as its RFI is OFF most of the time.

- 2) active (*A*): the device exchanges information with the coordinator. The RFI is continuously ON, which translates into high energy consumption.

The transition from state *I* to *A* occurs when a WuS is received from the coordinator, thus enabling the information exchange between the MTD and the coordinator. Upon receiving the WuS, the MTD goes to state *A*, either because it detected an event through its sensors and the coordinator granted a communication authorization (uplink grant) through the WuS, or because the WuS informs it of an imminent predicted event (request to transit to state *A*). The MTD stays at state *A* for the duration of the event.

The triggering events change the MTC traffic characteristics towards the coordinator. In Fig. 1, four MTDs are in state *A* (indicated with solid red arrows) and two are in state *I* (indicated with dashed green arrows). The MTDs wait for the WuS from the coordinator that would trigger state *A*. Note that according to the application, there are three elementary MTC traffic patterns [8]–[10]: periodic update, event-driven and payload exchange. Nevertheless, real world applications often combine these traffic types. Hence, considering the three elementary classes above enables building models with an arbitrary degree of complexity and accuracy [38]–[40].

Finally, we assume time is slotted in transmission time intervals (TTI). In slot  $k$  and state  $s \in \{I, A\}$ , MTDs generate traffic with rate  $R(k, s)$ , depending on their current state.

### III. TRAFFIC AND WAKE-UP MODELING

The traffic exchanged between the coordinator and the MTDs is modeled using an ergodic Markov chain with two states [47], *I* and *A*, as illustrated in Fig. 1. The payload exchange pattern is modeled through the  $q$  parameter in the geometric distribution. This parameter  $q$  considers how bursty could be the traffic generated by an event. A device goes to state *A* with probability

$$P_A = 1 - \exp\left(-2\pi\lambda_E \int_0^\infty p(d)\partial d\right). \quad (1)$$

Once in state *A*, the MTD remains there for a number  $k$  of TTIs, geometrically distributed with parameter  $q$ , thus, with probability mass function

$$f_K(k) = (1 - q)q^k, \quad k = 0, 1, \dots \quad (2)$$

The introduction of the additional parameter  $q$  in the Markov chain model allows tuning the temporal correlation of the individual rate processes of the MTDs and, as a result, that of the total rate process. Hence, the parameter  $q$  of the Markov chain enables tuning the model to suit various MTC applications and event reporting strategies. Furthermore, the parameter  $q$  can be used to study the impact of events on the temporal correlation of the total traffic at the coordinator. Focusing first on the case of small values of  $q$ , e.g.,  $q \leq 0.1$ , the traffic behaves similarly to a Bernoulli process (memoryless) [47], since it has a short memory. Increasing the value of  $q$  increases the memory, i.e., the total rate at a given time  $k$  is correlated with many past values. This is because once state *A* of the Markov chain is entered, one stays there longer [47].

We emphasize that, although modeled as in Fig. 1, the traffic that arrives to the coordinator has parameters that are different from the one seen by each MTD since the coordinator combines the traffic from several MTDs. In fact, the MTDs could have traffic patterns with parameters that are different from each other. For simplicity, we consider that the MTDs use a medium access control (MAC) technique to avoid collisions at the coordinator side. Since the proposed method focuses only on the coordinator, it is independent of the resolution of this problem at the MTD level and the additional complexity that this entails.

#### A. Wake-Up Scheme

Idle listening at the MTDs is avoided by leveraging WuS technology. The coordinator sends a WuS to opportunistically instruct the MTD that it must monitor for paging. Otherwise, the MTD skips the paging procedures, thus, it can potentially keep parts of its hardware switched off most of the time [17].

Fig. 3 depicts the different states and power consumption profiles for the proposed method as well as the benchmarks used for comparison purposes. Fig. 3 a) illustrates the DRX states as depicted in [30]. Notice that the level  $PW_1$  in DRX is not reached by any state. Conversely, the consumption in ON state is comparable with that in the active-decoding state even when no packet arrives. However, by using WuS, the device can activate a low-power beacon seeker whose consumption ( $PW_1$ ) saves energy with respect to the ON state in DRX, as shown in Fig. 3 b). Note that the MTD is allowed to traverse to a WRx-On state waiting for an active indicator within the aforementioned compact WuS (beacon) which reveals the PO ( $t_2$ ). Such beacon communicates to the MTD the necessity of commuting to a decoding state where the consumption is higher. This switching occurs at regular intervals and has a duration  $t_1$ , while the device remains in sleep state between them to save energy. At the end of the decoding state, if no more packets are to be exchanged, the device waits for an inactivity time ( $t_3$ ) before returning to the sleep state.

Observe that despite the potential decrease in power consumption triggered by a WuS scheme, some idle states may

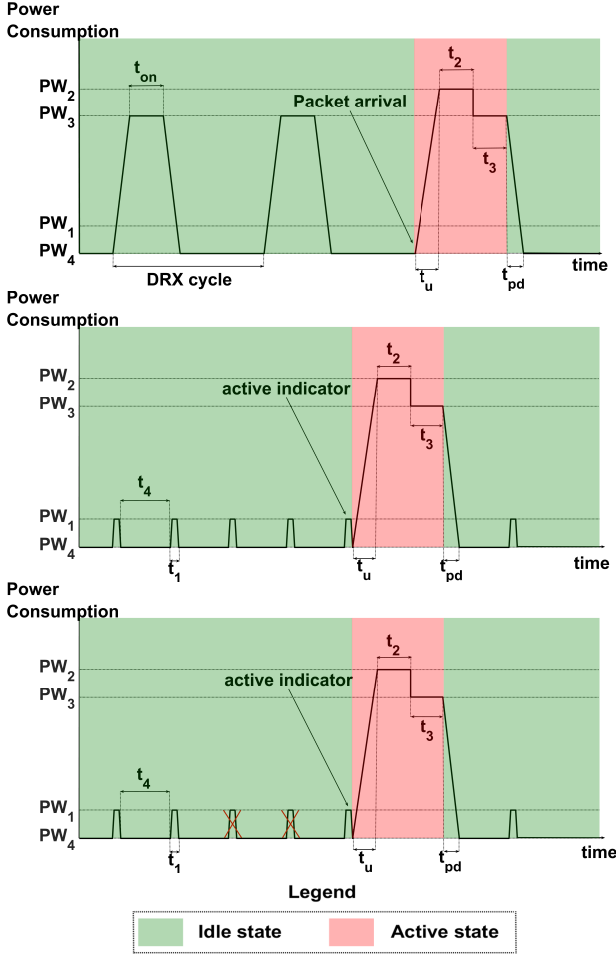


Fig. 3. Illustration of the different consumption profiles for the proposed and the benchmark schemes. a) DRX mechanism consumption profile as described in [30] (top), b) different wake up states and their respective power consumption (middle), and c) proposed FWuS, where turning ON the RFI during WRx-On events is avoided based on forecasting inter-arrival time (bottom). In case of a), PW1 is indicated only as a reference since this profile never works at this consumption level.

still occur where no WuS is detected. In this paper, we aim to avoid these states (marked with red crosses) based on a forecasting model, which is presented later in Section IV.

### B. Traffic Model

The transitions between wake-up states are modeled with a 4-state Markov chain as illustrated in Fig. 4.  $S_1$  represents the WRx-On, at which the MTD monitors PDWCH looking for a WuS alerting of a PO.  $S_2$  is the active-decoding state where the MTD decodes the information packets, while  $S_3$  represents the state for the inactivity timer. Finally,  $S_4$  corresponds to the sleep state in which the device is not able to receive any signal.

The MTD remains in state  $I$  for a time  $t_4$ , while switching to  $S_1$  immediately after. At  $S_1$ , the MTD monitors the channel searching for a WuS for a fixed time  $t_1$ . If the MTD detects a PO, it goes to  $S_2$  to decode the received information. If the whole information arrives before  $t_2$  ends, the MTD goes to  $S_3$ , otherwise  $t_2$  is reset and the MTD remains in  $S_2$ . At  $S_3$ , the device waits for a PO for a time  $t_3$  (inactivity timer). If a

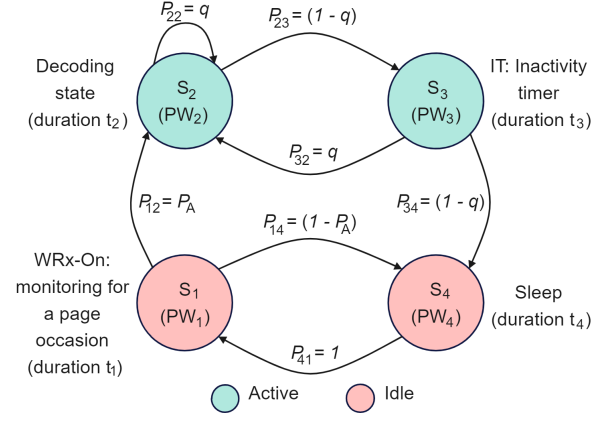


Fig. 4. The wake-up model as a semi-Markov chain.

scheduled PO is received within  $t_3$ , the MTD returns to  $S_2$ , otherwise it goes to  $S_4$  completing the wake-up cycle. Notice that the device consumes a start up time ( $t_u$ ) in transitions from  $S_1$  to  $S_2$ , and a power down time ( $t_{pd}$ ) from  $S_3$  to  $S_4$ . The transition probability from state  $S_i$  to  $S_j$  is denoted as  $P_{ij} = P(S_j|S_i)$  and also given in Fig. 4.

In this paper, we aim to optimally configure  $t_1$ ,  $t_2$ ,  $t_3$  and  $t_4$  as to minimize the energy consumption of the MTDs.

## IV. PROPOSED FWuS SCHEME

The traffic of most MTDs is substantially different from human traffic accessing the Internet [11]. In most IoT use cases, the traffic is either generated periodically, or as a burst after the detection of events [12]. Nonetheless, MTC traffic can be correlated in time and space [52]. This is because of the correlated temporal and spatial characteristics of a variety of events, e.g., low water or mineral concentration in crop soil and smart electricity metering. This sort of behavior can result in traffic bursts which can put stress on the receiver, e.g., the coordinator, since MTC traffic is usually uplink-dominated. It is therefore desirable to have tractable models that can be used to assess the impact of this type of traffic at the receiver [47].

In this context, accurate traffic prediction mechanisms are appealing, specially those relying on AI as they can potentially capture the inherent dynamics and non-linearities of the system [52]–[54]. Interestingly, long short-term memory (LSTM) is a popular type of recurrent NN (RNN) [55] that is specially designed to learn long-term dependencies of a sequence, thus, predictions are made based on long-sequences of previous input values rather than on a single previous input value [52], [56]. Different from classical solutions, e.g., relying on dynamic programming [57] and reinforcement learning [58], LSTM-based techniques [53], [59], [60] provide autonomous decision-making and relative fast learning speed, especially in problems with large state and action spaces.

We propose an LSTM-based traffic forecasting model and a methodology for properly configuring the WuS parameters. Note that an LSTM cell is made up of three gates, the input gate, the output gate and a forget gate. These gates determine if the information is read (input gate), if it is not relevant and is disregarded (forget gate), or if it is saved, impacting the current



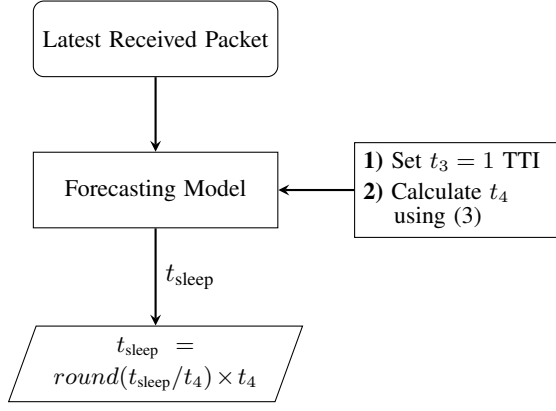


Fig. 5. Flowchart of the proposed WuS optimization,  $\text{round}(\cdot)$  represents the rounding operation to the nearest integer.

time step (output gate).<sup>1</sup> The inputs are the time-stamp of the latest packet ( $g_{o_i}$ ) and the latest relevant inter-arrival time, which are obtained via feedback. The inputs are modulated and used to train the unit. The forget gate contributes to dismiss over-training due to fluctuation in the training set. Then, a prediction for the next outcoming packet ( $g_{i+1}$ ) is obtained as output. As a result, we obtain a trained model for predicting the inter-arrival time between information packets using the known traffic data as input. Notice that the events that cause traffic data are independent among one another.

Recall that we aim to configure the WuS parameters as to minimize the MTDs' energy consumption based on the modeled traffic rate and the given application. Now, observe that  $t_3$  greatly impacts the energy consumption while the delay greatly depends on  $t_4$ . Tuning  $t_3$  and  $t_4$  to minimize the MTDs' energy consumption while maintaining a delay threshold is challenging since energy and delay are not jointly convex on  $t_3$  and  $t_4$ . Herein, we resort to setting the value of  $t_3$  to 1 TTI to assure low power consumption, while  $t_4$  is optimized in a way that allows satisfying a mean delay constraint ( $\bar{D}$ ):

$$t_4 = \max_{\substack{t_3=1 \text{ TTI} \\ D=\bar{D}}} \text{sleep}. \quad (3)$$

In (3),  $D$  is the packet delay and sleep is the time between every channel monitoring state ( $S_4$ ). Depending on the prediction, the system is able to decide whether to enter state  $S_1$  from  $S_4$  or not. Fig. 3 c) illustrates the proposed FWuS scheme, while Fig. 5 shows the proposed optimization flowchart. Once the WuS parameters are defined, they cannot be changed due to synchronization issues. However, we can extend  $S_4$  up to  $n \times t_4$  ( $\forall n = 1, 2, \dots$ ) as in Fig. 3 c). The system can dispense with WRx-On events, depending on the prediction, since it considers that the probability of a packet arriving is very low. Since the MTDs have limited processing power, the coordinator runs the forecasting model and configures the WuS parameters. Specifically,  $t_4$  is set according to (3), where  $t_{\text{sleep}}$  is predicted by the forecasting model based on the data. Notice that even when the proposed  $t_{\text{sleep}}$  is not

equal to  $t_4$ , the WuS parameters were prearranged between the coordinator and the MTDs. Therefore, in order to maintain the synchronism between the coordinator and each MTD, the time between  $T_{\text{ON}}$  beacons should be a multiple of  $t_4$ .

## V. PERFORMANCE METRICS

In this section, we discuss two performance metrics, named energy consumption and mean delay, which are utilized to assess the performance of the proposed method and to compare it with the benchmarks. We find expressions for these metrics based on the Markov chain in Fig. 4 for a given WuS configuration. Additionally, to confirm the accuracy of the predictor, we calculate the root mean square error (RMSE) between the estimated ( $g_i$ ) and actual ( $g_{o_i}$ ) inter-arrival values,

$$\text{RMSE} = \sqrt{\frac{1}{M} \sum_{i=1}^M (g_i - g_{o_i})^2}, \quad (4)$$

where  $M$  is the sample size. Moreover, the fitting performance is validated and tested using the R metric, defined as

$$R = \sqrt{1 - \frac{1}{M} \sum_{i=1}^M \left(1 - \frac{g_i}{g_{o_i}}\right)^2}. \quad (5)$$

This statistic measures how successful the fit is in explaining the variation of the data. Therefore, it represents the correlation between the actual values and the predicted ones. In general, the higher the R metric is, the better the model fits the data.

### A. Energy Consumption

In this paper, we adopt a simplified model based on [37] that refers only to the energy consumption of the RFI, i.e.,  $\text{PW}_4 = 0$ . Based on Fig. 3, which shows the power consumption levels ( $\text{PW}_i$ ) for every WuS state  $S_i$ ,  $i = (1, 2, 3, 4)$ , the mean power consumption ( $\bar{\text{PW}}$ ) is calculated as

$$\bar{\text{PW}} = \frac{\sum_{i=1}^4 p_i t_i \text{PW}_i + \frac{1}{2} (p_1 P_{12} t_u \text{PW}_2 + p_3 P_{34} t_{pd} \text{PW}_3)}{p_1 P_{12} t_u + p_3 P_{34} t_{pd} + \sum_{i=1}^4 p_i t_i}, \quad (6)$$

where  $p_i$  denotes the probability of being in state  $S_i$ . Thus, by exploiting  $p_i = \sum_{j=1}^4 p_j P_{ji}$ ,  $\sum_{i=1}^4 p_i = 1$ , and the semi-Markov chain in Fig. 4, we obtain

$$p_1 = p_4 = \frac{(q-1)^2}{L}, \quad p_2 = \frac{P_A}{L}, \quad p_3 = \frac{P_A(1-q)}{L}. \quad (7)$$

where  $L = 2P_A - 4q - qP_A + 2q^2 + 2$ .

The time the device spends in each state, multiplied by its corresponding power consumption, over the total time, outputs the mean power consumption. Moreover, the time to reach the state could be dismissed except for the start up time ( $t_u$ ) and the power down time ( $t_{pd}$ ), whose values are large enough to be considered. The power consumption in these transitions is approximated, without losing generality, by their triangle geometrical format (see Fig. 3), leading to the 1/2 coefficient in (6).

<sup>1</sup>Interested readers in the details of LSTM networks are advised to review [56], [61].

### B. Delay Constraints

We assume that a packet experiences delay only when the situation that generates the detection of a triggering event finds the MTD in sleep ( $S_4$ ) or WRx-On ( $S_1$ ) state. This is because in active ( $S_2$ ) and inactivity timer ( $S_3$ ) states, the exchange of information with the coordinator is immediate. Then,  $\bar{D}$  can be estimated as

$$\bar{D} = p_A P_A \left( 3(t_u + t_1) + \frac{t_4^2}{2} + \sum_{n=1}^{\infty} p_{md}^n t_4 \right) + t_{mac}. \quad (8)$$

Packets experience delay in 3 cases:

- 1) a packet is intended to be delivered while the RFI of the MTD is at  $S_1$ . In this case, the packet experiments a delay  $t_u + t_1$ ;<sup>2</sup>
- 2) a packet is buffered on hold while the RFI of the MTD is at  $S_4$  state. Then, the experienced delay is given by  $t_u + t_1 + \int_0^{t_4} t \partial t = t_u + t_1 + t_4^2/2$ ;
- 3) the MTD does not receive the PO scheduled for information exchange, thus, there is a miss-detection. In this case, the device has to wait until the next PO, and the packet experiences a delay  $t_u + t_1 + \sum_{n=1}^{\infty} p_{md}^n t_4$ . Herein,  $p_{md}$  represents the miss detection probability and  $n$  is the number of lost POs.

The mean delay also includes a term  $t_{mac}$  that comprises the delay introduced by the MAC scheme aiming at avoiding/solving collisions. We assume that the communication requirements could be met with a suitable MAC algorithm.

### C. Power Saving Factor

Finally, we calculate the relative power saving ( $\eta$ ) regarding a benchmark, thus, it quantifies the amount of energy that can be saved by implementing our proposed scheme. This power saving factor is calculated as

$$\eta = \frac{\overline{PW}_b - \overline{PW}}{\overline{PW}_b}, \quad (9)$$

where  $\overline{PW}_b$  represents the power consumption of the benchmark scheme and is calculated using (6) with the values respective to the benchmark.

## VI. NUMERICAL RESULTS

In this section, we evaluate the performance of the proposed method. Without losing generality, we assume a negative exponential function to model the influence of events on the traffic of the MTDs, i.e.,  $p(d) = e^{-d}$ . The MTDs are deployed with density  $\lambda_M = 10^{-1}$  (MTDs/ $m^2$ ), and TTI is assumed equal to 1 ms. All devices are at the state  $I$  at the beginning of the simulation. These parameters are set for all the numerical results unless specified otherwise.

<sup>2</sup>In practice,  $t_u$  dominates here due to the very small values of  $t_1$ .

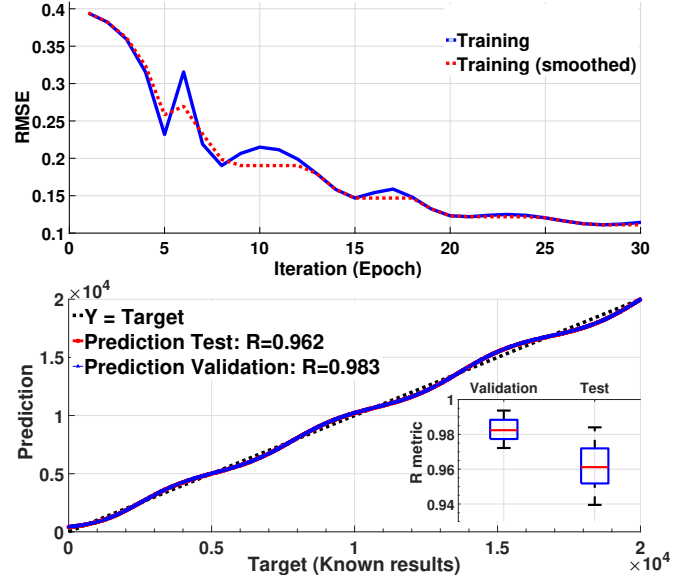


Fig. 6. Training and validation process of the forecasting model. a) RMSE values during training process for 30 epochs (top), b) validation and test processes (bottom). The latter shows the correspondence between predicted and known results. The dotted black line shows the ideal scenario where the predicted and known results match.

### A. Benchmarks

As benchmarks, we resort to the WuS scheme in [37], and the optimized DRX-based reference mechanism in [30]. The scheme in [37] models a standard WuS behavior (see Fig. 3 b)). In this scheme, the time interval between WRx-On states ( $S_1$ ) is predefined in a static and invariable way. The configuration values of the WuS scheme come from [37]. Meanwhile, the basic operation and representative power consumption behavior of the DRX-enabled conventional cellular module [30] is shown in Fig. 3 a). Observe that the RFI remains ON for a time  $t_{on}$ , during which the MTD is waiting to receive information packets. If during this time no packets are received, the RFI goes to the OFF state, completing the DRX cycle. This cycle is repeated until a data packet is received, after which the system goes to the active-decoding state with duration  $t_2$ . Then, the inactivity timer is activated for a time  $t_3$ . If packets are received in this state, the MTD returns to the active-decoding state, otherwise, it goes to the OFF state. In every case, the process is repeated.

In state A, the consumption is higher than in the other states ( $PW_2$ ). In the inactivity timer state and in the ON state of the DRX cycle, the consumption is equal to  $PW_3$ . In the OFF state of the DRX cycle, the consumption is  $PW_4$ . Note that the DRX cycle consists of a time in the ON state plus a time in the OFF state. The DRX configuration values are taken from [30].

### B. Simulation Framework

We use the traffic model in Section III-B to simulate several log traces of traffic received at the coordinator. In each log trace, the deployment of the MTDs and event epicenters is generated according to the corresponding PPP. We consider the

TABLE IV  
SIMULATION PARAMETERS

Parameter	Value	Ref.
$t_1$	1/14 (TTI)	[37]
$t_2$	1 (TTI)	[37]
$t_3$	1 (TTI)	[37]
$t_u$	15 (TTI)	[37]
$t_{pd}$	10 (TTI)	[37]
$\bar{D}$	30 ms	
$PW_1$	57 mW	[37]
$PW_2$	935 mW	[37]
$PW_3$	850 mW	[37]
$PW_4$	$\approx 0$ mW	[37]
$\lambda_E$	$10^{-5}, 10^{-4}, 10^{-3}, 10^{-2}$	[47]
$\lambda_M$	$10^{-1}$ (MTD/ $m^2$ )	[47]
$p(d)$	$e^{-d}$	[47]
$q$	[0.1, 0.9]	
$t_{on}$	1 (TTI)	[30]
$p_{md}$	0.01	[37]
$p_f$	0.1	[37]

influence of each event epicenter on the MTDs via  $p(d)$ . The latter influences  $P_A$  in the traffic model through (1). The events are independent among one another. These traffic data are then used as input of the LSTM network to train the forecasting model. Specifically, 70% of the sample data is used to perform training, 15% for the validation set, while the remaining 15% for the testing set. For the training, validation, and testing process,  $9.8 \times 10^4$ ,  $2.1 \times 10^4$ , and  $2.1 \times 10^4$  information packets were respectively processed, thus making a total of  $1.4 \times 10^5$ . The LSTM architecture is configured with 1 hidden layer (100 Neurons), ‘Initial Learn Rate’ equal to 0.0001, RMSE loss function, maximum 50 epochs [62], [63], and using the Adam optimizer [64]. Note that the LSTM’s learning algorithm is local in space and time, while its computational complexity per time step and weight is  $O(1)$  [61], thus, leading to a system complexity  $O(2 \times 100)$ .

The traffic forecasting model is then used to optimize the WuS parameters. Specifically, the coordinator is configured with a standard WuS behavior (see Fig. 3 b)). Values of WuS parameters are obtained from [37], while the value for  $t_4$  is re-calculated using the framework in [37] for our system and traffic models aiming to be fair in the comparison. Lastly, we provide the coordinator RFI with the optimized DRX-based reference mechanism in [30], as suggested by [37]. The DRX cycle values are adapted according to our traffic model. In this case,  $t_{on}$  is established equal to 1 TTI in order to save energy, while  $t_u$ ,  $t_{pd}$ ,  $t_2$  and  $t_3$  have common values for each method.

Table IV summarizes the parameters used in the simulation process. We calculate  $t_4$  (sleep time) using (3) and (8). All simulations were carried out in Matlab<sup>®</sup> [65]. The illustrated curves are the result of Monte Carlo simulations over 150 runs, where the position of the MTDs and the events’ epicenter are randomly distributed in each run.

### C. Prediction Accuracy

Fig. 6 a) illustrates the performance of the forecasting training process. Note that after 30 epochs, the RMSE value remains approximately constant at around 0.1. In the validation

and test processes, the obtained R values were above 96%, demonstrating high accuracy to adapt to incoming data. In addition, Fig. 6 b) shows the statistics on the accuracy of the predictor over 150 runs. The standard deviation for validation and test processes are 1.09% and 2.27%, respectively. The obtained confusion table is as follows

WRx-On	Prediction	
	True	False
Positive	91.2%	8.8%
Negative	98.7%	1.3%

Notice that miss-detection probability is actually the false negative probability, while the false alarm probability is actually the probability of taking a false positive. Then, by adjusting these values, we are indirectly adjusting the accuracy of the predictor model. In this case, less than 10% (8.8%) of the energy saving opportunities are missed, while the risk for late activation is just 1.3%. Note that a deeper LSTM architecture or more training epochs would enhance the prediction accuracy but it would increase complexity and time of training as well.

### D. Delay and Power Consumption Performance

Fig. 7 a) and b) illustrate the required delay and power consumption, respectively, as a function of predictor’s accuracy. The latter is given in terms of miss-detection probability (probability that the MTD misses a PO or WuS) and the false alarm probability (probability that the MTD receives a PO or WuS needlessly, i.e., when there is no information to transmit/receive). As observed in Fig. 7 a), the false alarm probability has no impact on the delay, while the miss-detection probability increases less than 15% (4.3 ms) and 5% (1.4 ms) for values below 0.1 and 0.05, respectively. As for the power consumption, Fig. 7 b) evinces the tremendous impact of the false alarm probability, while decreasing the miss-detection probability below 0.4 has almost no impact. In this paper, the maximum values of miss-detection and false alarm probabilities, which serve as constraints to the forecasting model, are adjusted to 0.01 and 0.1, respectively.

Fig. 8 depicts the power consumption as a function of the number of MTDs for each scheme. In case of Fig. 8 a), we consider event densities  $\lambda_E \in \{10^{-5}, 10^{-2}\}$ , while each MTD is randomly assigned a value of  $q \in [0, 1]$ . Note that our proposed scheme outperforms all the others, while the energy saving with respect to WuS [37] becomes even greater as the traffic volume increases. To generalize and better illustrate this, we adopt a different event density in Fig. 8 b), as well as different values for  $q$ . Note that the range of  $q$  was varied with the aim of testing more/less bursty traffic patterns. In all the cases, the energy consumption under the proposed scheme is considerably lower with respect to WuS [37] and DRX [30]. Interestingly, FWuS saves energy independently of the number of served MTDs under low bursty traffic, while DRX and WuS lead to the same power consumption regardless of the type of traffic when serving 5 to 7 MTDs. Thus, the power consumption increases with both the number of served MTDs and  $q$ . For small  $q$ , the increase of the power consumption with the number of MTDs is smooth, while as  $q$  increases, there might be sudden jumps in power consumption.



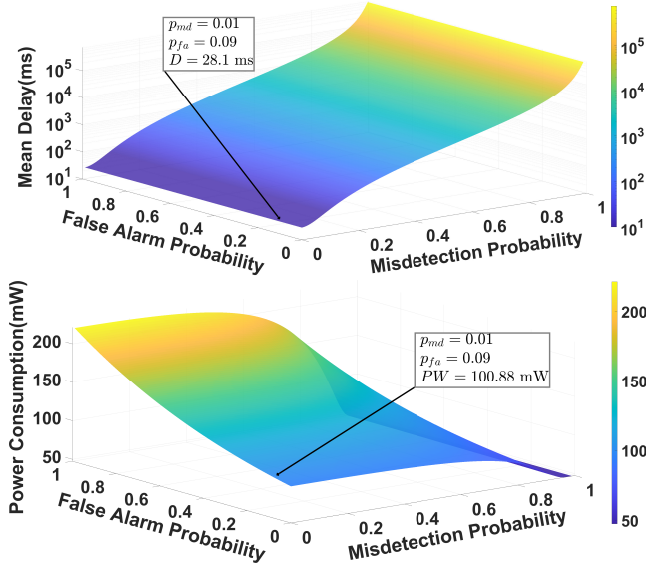


Fig. 7. System behavior regarding variations in miss-detection and false alarm probabilities: a) mean delay (top) and b) power consumption (bottom). The marker represents the operation point of our forecasting model.

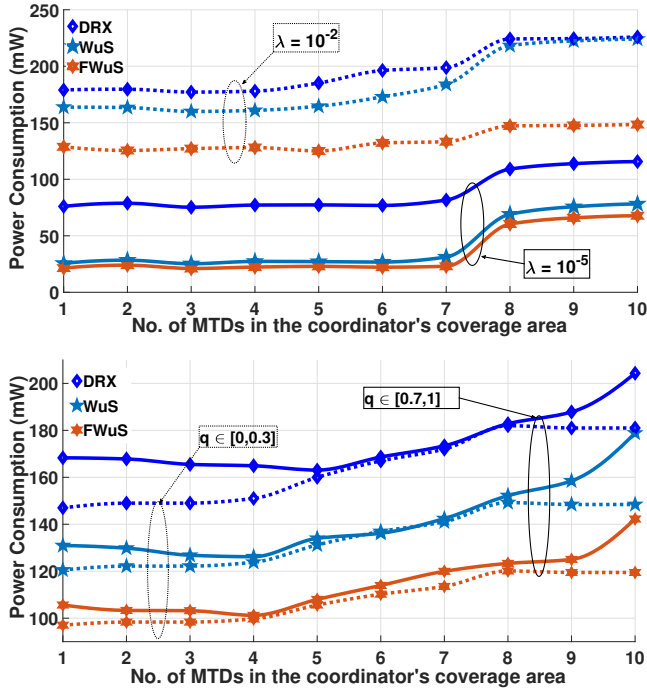


Fig. 8. Power consumption analysis as a function of the number of MTDs in the coordinator's coverage area. a)  $\lambda_E \in \{10^{-5}, 10^{-2}\}$  and  $q \in [0, 1]$  (top), b)  $\lambda_E = 10^{-3}$  and  $q \in \{[0, 0.3], [0.7, 1]\}$ , respectively (bottom).

Note that since the power consumption becomes greater as the number of MTDs increases, the performance figures corresponding to 1 and 10 MTDs are relevant/representative. Hence, we characterize in more detail the power consumption performance for such numbers of MTDs in Table V. Here,  $\overline{PW}$ ,  $PW_{\max}$ , and  $PW_{\min}$  represent the mean, maximum and minimum power consumption over the 150 Monte Carlo runs, while std is the standard deviation.

TABLE V  
POWER CONSUMPTION (mW) FOR 1 MTD (WHITE) AND 10 MTDs (LIGHTGRAY)

Parameters		Results			
$\lambda_E$	$q$	$\overline{PW}$	$PW_{\max}$	$PW_{\min}$	std
$10^{-5}$	$[0, 1]$	21.423	23.594	18.356	2.671
		67.738	76.061	59.164	8.602
$10^{-2}$	$[0, 1]$	127.723	142.143	112.712	13.915
		149.859	154.113	134.215	14.212
$10^{-3}$	$[0, 0.3]$	97.023	110.468	83.182	12.366
		119.461	130.972	107.041	11.667
$10^{-3}$	$[0.7, 1]$	105.603	120.091	93.889	9.659
		142.239	152.112	131.943	9.011

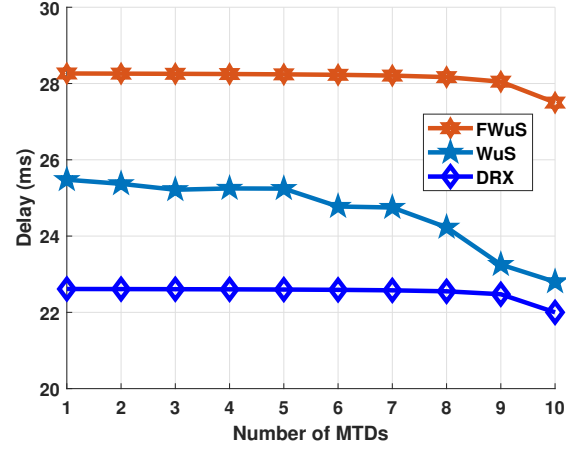


Fig. 9. Delay analysis as a function of the number of MTDs handled by the coordinator. Maximum variations of +1.4 ms and -2.1 ms, with 'std' equal to 1.1 ms when the number of MTDs is 10.

Fig. 9 illustrates the mean delay experienced by each scheme. Notice that in all cases the delay is below the constraint of 30 ms, and the performance gap between our proposal and WuS [37] is between 3 and 5 ms, while the gap regarding DRX [30] increases up to 6 ms. Notice that this figure illustrates the maximum mean delay when varying the event density between  $\{10^{-5}, 10^{-4}, 10^{-3}, 10^{-2}\}$ , thus representing the worst-case scenario for the mean delay.

#### E. Power Saving and Dynamic Adjustment

Table VI illustrates the relative power saving ( $\eta$ ) regarding WuS [37]. In this case, we analyze the amount of energy that can be saved by implementing our proposed scheme instead of WuS, and quantify its dispersion via the std metric. Notice that we use WuS [37] as it is more energy efficient than DRX [30]. Evidently, the proposed FWuS saves much more energy than WuS [37], especially under high density of events and/or MTDs. Savings in energy consumption go from 10% to around 20% for low-density event scenarios. Meanwhile, the savings increase up to almost 35% for high-density event scenarios, thus guaranteeing good performance despite harsh scenario dynamics.

Fig. 10 illustrates the performance of FWuS when the events density varies dynamically over a period of time. This is completely different from the approaches in sections VI-C and VI-D, where these parameters were completely deterministic.

TABLE VI  
RELATIVE POWER SAVING ( $\eta$ )

Parameters			Results		
$\lambda_E$	$q$	$\bar{\eta}$	$\eta_{\max}$	$\eta_{\min}$	std
$10^{-5}$	[0, 1]	16.4%	26.3%	12.6%	4.2%
$10^{-2}$	[0, 1]	28.41%	34.2%	22.9%	4.9%
$10^{-3}$	[0, 0.3]	19.33%	21.3%	16.8%	2.3%
$10^{-3}$	[0.7, 1]	19.5%	22.3%	15.8%	2.7%

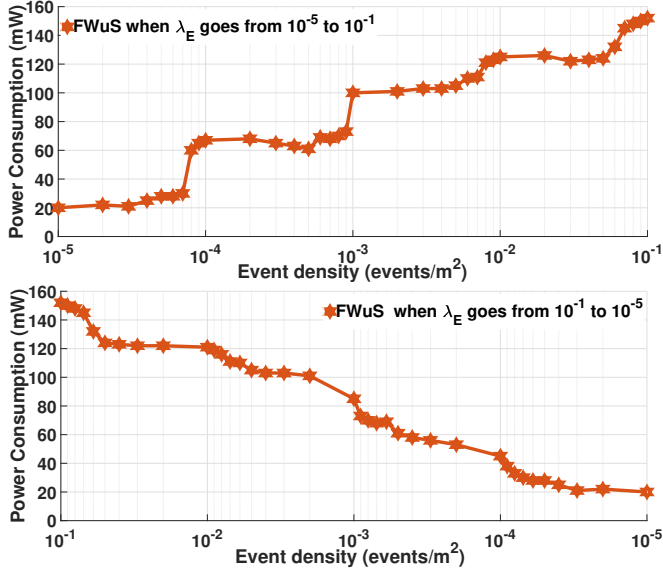


Fig. 10. Energy consumption analysis when the event density changes dynamically throughout a period of time. a)  $\lambda_E$  from  $10^{-5}$  to  $10^{-1}$  (top), and b)  $\lambda_E$  from  $10^{-1}$  to  $10^{-5}$  (bottom).

Specifically, events density increases from  $10^{-5}$  to  $10^{-1}$  in Fig. 10 a), and decreases from  $10^{-1}$  to  $10^{-5}$  in Fig. 10 b). Note that the variations in event density change the activation probability of the MTDs, thus leading to changes in traffic patterns and challenging the online predictor. Nevertheless, the proposed scheme is able to adapt itself to these variations. Interestingly, the system adapts more smoothly when the event density decreases since the scheme has more freedom to predict covered by the false alarm and miss-detection probabilities that adapt better to the decrease in traffic than to its increase. Meanwhile, abrupt power consumption peaks may appear when the event density increases due to the loss of multiple energy-saving opportunities caused by the restriction imposed by the miss-detection probability target.

## VII. CONCLUSIONS

In this paper, we considered an MTC network controlled by a single coordinator. We modeled the location of MTDs and event epicenters as independent PPPs, while considering event-driven traffic patterns with geometrically distributed burst duration. We proposed an intelligent wake-up scheme (FWuS) to be used by the coordinator to reduce the energy consumption in the MTDs and prolong their battery lifetime. Specifically, FWuS exploits an accurate traffic forecasting model that optimizes the wake-up parameters, thus, favouring energy

savings. The traffic forecasting relies on a simple LSTM neural network, which achieves prediction accuracy results above 96% by monitoring the MTC traffic patterns. Numerical results evinced that the proposed FWuS enables energy consumption reduction up to almost 35% to the competing scheme with the best performance, while the mean delay increases only 2–6 ms but is always below the 30 ms constraint. Moreover, the proposed mechanism was shown to be robust/adaptable to scenario/traffic with dynamically changing parameters, performing well under traffic variability.

Some interesting research directions to pursue in the sequence are: i) considering/exploiting the traffic correlation between nearby MTDs that potentially detect the same events to avoid transmission of unnecessary redundant traffic, thus saving energy; ii) controlling the duration and restart procedure of the inactivity timer, e.g., via downlink control information, which seems appealing to reduce the active time; and iii) analyzing/comparing predictors' efficiency in terms of complexity and accuracy trade-offs, including more demanding scenarios such as those with 'on device intelligence'. Finally, acquiring and exploiting data from the industry, while validating the proposed mechanisms, is a goal for future work.

## REFERENCES

- [1] N. H. Mahmood, S. Böcker, I. Moerman, O. A. López, A. Munari, K. Mikhaylov, F. Clazzer, H. Bartz, O.-S. Park, E. Mercier *et al.*, "Machine type communications: key drivers and enablers towards the 6G era," *EURASIP Journal on Wireless Communications and Networking*, vol. 2021, no. 1, pp. 1–25, 2021.
- [2] J. Ding, M. Nemati, C. Ranaweera, and J. Choi, "IoT Connectivity Technologies and Applications: A Survey," *IEEE Access*, vol. 8, pp. 67 646–67 673, 2020.
- [3] N. Xia, H.-H. Chen, and C.-S. Yang, "Emerging Technologies for Machine-Type Communication Networks," *IEEE Network*, vol. 34, no. 1, pp. 214–222, 2019.
- [4] G. A. Akpakwu, B. J. Silva, G. P. Hancke, and A. M. Abu-Mahfouz, "A survey on 5G networks for the Internet of Things: Communication technologies and challenges," *IEEE Access*, vol. 6, pp. 3619–3647, 2017.
- [5] G. Manogaran, G. Srivastava, B. A. Muthu, S. Baskar, P. M. Shakeel, C.-H. Hsu, A. K. Bashir, and P. M. Kumar, "A response-aware traffic offloading scheme using regression machine learning for user-centric large-scale Internet of Things," *IEEE Internet of Things Journal*, vol. 8, no. 5, pp. 3360–3368, 2020.
- [6] X. Yan and M. Ma, "A Privacy-Preserving Handover Authentication Protocol for a Group of MTC Devices in 5G Networks," *Computers & Security*, p. 102601, 2022. [Online]. Available: <https://www.sciencedirect.com/science/article/pii/S0167404821004247>
- [7] F. Luo, X. Sun, W. Zhan, J. Zou, and H. Tan, "Distributed Delay Optimization of Machine-Type Communications in 5G Networks," in *Computing, Communications and IoT Applications (ComComAp)*, 2021, pp. 138–143.
- [8] A. Zanella, N. Bui, A. Castellani, L. Vangelista, and M. Zorzi, "Internet of Things for smart cities," *IEEE Internet of Things journal*, vol. 1, no. 1, pp. 22–32, 2014.
- [9] R. Bayindir, E. Hossain, and S. Vadi, "The path of the smart grid-the new and improved power grid," in *International Smart Grid Workshop and Certificate Program (ISGWCP)*. IEEE, 2016, pp. 1–8.
- [10] R. Ratasuk, A. Prasad, Z. Li, A. Ghosh, and M. A. Uusitalo, "Recent advancements in M2M communications in 4G networks and evolution towards 5G," in *18th International Conference on Intelligence in Next Generation Networks*. IEEE, 2015, pp. 52–57.
- [11] J. Wu, B. Yang, L. Wang, and J. Park, "Adaptive DRX Method for MTC Device Energy Saving by Using a Machine Learning Algorithm in an MEC Framework," *IEEE Access*, vol. 9, pp. 10 548–10 560, 2021.
- [12] J. Zhou, G. Feng, T.-S. P. Yum, M. Yan, and S. Qin, "Online Learning-Based Discontinuous Reception (DRX) for Machine-Type Communications," *IEEE Internet of Things Journal*, vol. 6, no. 3, pp. 5550–5561, 2019.

- [13] Y.-N. R. Li, M. Chen, J. Xu, L. Tian, and K. Huang, "Power Saving Techniques for 5G and Beyond," *IEEE Access*, vol. 8, pp. 108 675–108 690, 2020.
- [14] A. A. Benbuk, N. Kouzayha, J. Costantine, and Z. Dawy, "Tunable, Asynchronous, and Nanopower Baseband Receiver for Charging and Wake-up of IoT Devices," *IEEE Internet of Things Journal*, 2021.
- [15] M. Shehab, A. K. Hagelskjær, A. E. Kalør, P. Popovski, and H. Alves, "Traffic Prediction Based Fast Uplink Grant for Massive IoT," in *IEEE 31st Annual International Symposium on Personal, Indoor and Mobile Radio Communications*. IEEE, 2020, pp. 1–6.
- [16] W. Zhan, C. Xu, X. Sun, and J. Zou, "Toward Optimal Connection Management for Massive Machine-Type Communications in 5G System," *IEEE Internet of Things Journal*, vol. 8, no. 17, pp. 13 237–13 250, 2021.
- [17] J. Dian and R. Vahidnia, "LTE IoT Technology Enhancements and Case Studies," *IEEE Consumer Electronics Magazine*, 2020.
- [18] N. Mazloum and O. Edfors, "Interference-free OFDM embedding of wake-up signals for low-power wake-up receivers," *IEEE Transactions on Green Communications and Networking*, vol. 4, no. 3, pp. 669–677, 2020.
- [19] 3GPP, "TS38. 300: NR; NR & NG-RAN overall description; Stage 2," 2019.
- [20] *Draft Standard for Information Technology–Telecommunications and Information Exchange Between Systems–Local and Metropolitan Area Networks–Specific Requirements Part 11: Wireless LAN Medium Access Control (MAC) and Physical Layer (PHY) Specifications–Amendment 9: Wake-Up Radio Operation*, Standard IEEE P802.11ba, Jun. 2020.
- [21] E. Stepanova, D. Bankov, E. Khorov, and A. Lyakhov, "On the Joint Usage of Target Wake Time and 802.11 ba Wake-Up Radio," *IEEE Access*, vol. 8, pp. 221 061–221 076, 2020.
- [22] T. J. Odelberg, J. Im, and D. D. Wentzloff, "A 2.1 mW- 109dBm NB-IoT Wake-Up Receiver," in *IEEE Radio Frequency Integrated Circuits Symposium (RFIC)*. IEEE, 2021, pp. 235–238.
- [23] 3GPP, "TS 36.211, Section 10.2.6B; Narrowband Wake Up Signal."
- [24] Y. Mafi, F. Amirhosseini, S. A. Hosseini, A. Azari, M. Masoudi, and M. Vaezi, "Ultra-Low-Power IoT Communications: A novel address decoding approach for wake-up receivers," *IEEE Transactions on Green Communications and Networking*, pp. 1–1, 2021.
- [25] K. Heins, "NB-IoT Network Deployment," in *NB-IoT Use Cases and Devices*. Springer, 2022, pp. 81–86.
- [26] A. Froytlog, T. Foss, O. Bakker, G. Jevne, M. A. Haglund, F. Y. Li, J. Oller, and G. Y. Li, "Ultra-low power wake-up radio for 5G IoT," *IEEE Communications Magazine*, vol. 57, no. 3, pp. 111–117, 2019.
- [27] J. Oller, I. Demirkol, J. Casademont, J. Paradells, G. U. Gamm, and L. Reindl, "Has time come to switch from duty-cycled MAC protocols to wake-up radio for wireless sensor networks?" *IEEE/ACM Transactions on Networking*, vol. 24, no. 2, pp. 674–687, 2015.
- [28] M. Magno, V. Jelicic, B. Sribnovski, V. Bilas, E. Popovici, and L. Benini, "Design, implementation, and performance evaluation of a flexible low-latency nanowatt wake-up radio receiver," *IEEE Transactions on Industrial Informatics*, vol. 12, no. 2, pp. 633–644, 2016.
- [29] K. Zhou, N. Nikaein, and T. Spyropoulos, "LTE/LTE-A Discontinuous Reception Modeling for Machine Type Communications," *IEEE Wireless Communications Letters*, vol. 2, no. 1, pp. 102–105, 2013.
- [30] H. Ramazanali and A. Vinel, "Tuning of LTE/LTE-A DRX parameters," in *IEEE 21st International Workshop on Computer Aided Modelling and Design of Communication Links and Networks (CAMAD)*. IEEE, 2016, pp. 95–100.
- [31] S. Huang, G. Feng, L. Liang, and S. Qin, "Power-saving coercive sleep mode for machine type communications," in *23rd Asia-Pacific Conference on Communications (APCC)*, 2017, pp. 1–6.
- [32] H.-L. Chang and M.-H. Tsai, "Optimistic DRX for Machine-Type Communications in LTE-A Network," *IEEE Access*, vol. 6, pp. 9887–9897, 2018.
- [33] J. Guo, Y. Chen, J. Zhu, and S. Zhang, "Can We Achieve Better Wireless Traffic Prediction Accuracy?" *IEEE Communications Magazine*, vol. 59, no. 8, pp. 58–63, 2021.
- [34] N. M. Balasubramanya, L. Lampe, G. Vos, and S. Bennett, "On Timing Reacquisition and Enhanced Primary Synchronization Signal (ePSS) Design for Energy Efficient 3GPP LTE MTC," *IEEE Transactions on Mobile Computing*, vol. 16, no. 8, pp. 2292–2305, 2017.
- [35] J. Rinne, J. Keskinen, P. R. Berger, D. Lupo, and M. Valkama, "Viability Bounds of M2M Communication Using Energy-Harvesting and Passive Wake-Up Radio," *IEEE Access*, vol. 5, pp. 27 868–27 878, 2017.
- [36] S. Rostami, K. Heiska, O. Puchko, K. Leppanen, and M. Valkama, "Wireless powered wake-up receiver for ultra-low-power devices," in *IEEE Wireless Communications and Networking Conference (WCNC)*. IEEE, 2018, pp. 1–5.
- [37] S. Rostami, S. Lagen, M. Costa, M. Valkama, and P. Dini, "Wake-Up Radio Based Access in 5G Under Delay Constraints: Modeling and Optimization," *IEEE Transactions on Communications*, vol. 68, no. 2, pp. 1044–1057, 2019.
- [38] E. Eldeeb, M. Shehab, and H. Alves, "A Learning-Based Fast Uplink Grant for Massive IoT via Support Vector Machines and Long Short-Term Memory," *IEEE Internet of Things Journal*, 2021.
- [39] N. Nikaein, M. Laner, K. Zhou, P. Svoboda, D. Dragic, M. Popovic, and S. Krco, "Simple Traffic Modeling Framework for Machine Type Communication," in *The Tenth International Symposium on Wireless Communication Systems*, 2013, pp. 1–5.
- [40] O. L. López, N. H. Mahmood, H. Alves, and M. Latva-aho, "CSI-free vs CSI-based multi-antenna WET for massive low-power Internet of Things," *IEEE Transactions on Wireless Communications*, vol. 20, no. 5, pp. 3078–3094, 2021.
- [41] O. Teyeb, A. Muhammad, G. Mildh, E. Dahlman, F. Barac, and B. Makki, "Integrated Access Backhauled Networks," in *IEEE 90th Vehicular Technology Conference (VTC2019-Fall)*, 2019, pp. 1–5.
- [42] A. Abdrabou, M. Al Darei, M. Prakash, and W. Zhuang, "Application-Oriented Traffic Modeling of WiFi-based Internet of Things Gateways," *IEEE Internet of Things Journal*, 2021.
- [43] G. C. Madueno, Č. Stefanović, and P. Popovski, "Reliable and efficient access for alarm-initiated and regular M2M traffic in IEEE 802.11 ah systems," *IEEE Internet of Things Journal*, vol. 3, no. 5, pp. 673–682, 2015.
- [44] S. Rostami, S. Lagen, M. Costa, P. Dini, and M. Valkama, "Optimized wake-up scheme with bounded delay for energy-efficient MTC," in *IEEE Global Communications Conference (GLOBECOM)*. IEEE, 2019, pp. 1–6.
- [45] J. Sachs, G. Wikstrom, T. Dudda, R. Baldemair, and K. Kittichokechai, "5G radio network design for ultra-reliable low-latency communication," *IEEE network*, vol. 32, no. 2, pp. 24–31, 2018.
- [46] M. Mahlouji and T. Mahmoodi, "Analysis of Uplink Scheduling for Haptic Communications," in *IEEE Globecom Workshops (GC Wkshps)*. IEEE, 2018, pp. 1–7.
- [47] H. Thomsen, C. N. Manchón, and B. H. Fleury, "A traffic model for machine-type communications using spatial point processes," in *IEEE 28th Annual International Symposium on Personal, Indoor, and Mobile Radio Communications (PIMRC)*. IEEE, 2017, pp. 1–6.
- [48] Y. Chen, J. Yang, X. Cao, and S. Zhang, "Energy efficiency optimization for heterogeneous cellular networks modeled by Matérn hard-core point process," *China Communications*, vol. 17, no. 8, pp. 70–80, 2020.
- [49] N. Deng and M. Haenggi, "The Energized Point Process as a Model for Wirelessly Powered Communication Networks," *IEEE Transactions on Green Communications and Networking*, vol. 4, no. 3, pp. 832–844, 2020.
- [50] F. Li and K.-Y. Lam, "Resource optimization in satellite-based Internet of Things," in *International Conference on Artificial Intelligence in Information and Communication (ICAIIIC)*. IEEE, 2020, pp. 006–011.
- [51] X. Zhang, J. Grajal, M. López-Vallejo, E. McVay, and T. Palacios, "Opportunities and challenges of ambient radio-frequency energy harvesting," *Joule*, vol. 4, no. 6, pp. 1148–1152, 2020.
- [52] K. He, X. Chen, Q. Wu, S. Yu, and Z. Zhou, "Graph Attention Spatial-Temporal Network With Collaborative Global-Local Learning for Citywide Mobile Traffic Prediction," *IEEE Transactions on Mobile Computing*, vol. 21, no. 4, pp. 1244–1256, 2022.
- [53] S. Mahajan, H. R., and K. Kotecha, "Prediction of Network Traffic in Wireless Mesh Networks Using Hybrid Deep Learning Model," *IEEE Access*, vol. 10, pp. 7003–7015, 2022.
- [54] Z. Zhang, F. Li, X. Chu, Y. Fang, and J. Zhang, "dmTP: A Deep Meta-Learning Based Framework for Mobile Traffic Prediction," *IEEE Wireless Communications*, vol. 28, no. 5, pp. 110–117, 2021.
- [55] J. Wang, J. Tang, Z. Xu, Y. Wang, G. Xue, X. Zhang, and D. Yang, "Spatiotemporal modeling and prediction in cellular networks: A big data enabled deep learning approach," in *IEEE INFOCOM - IEEE Conference on Computer Communications*. IEEE, 2017, pp. 1–9.
- [56] M. L. Memon, M. K. Maheshwari, N. Saxena, A. Roy, and D. R. Shin, "Artificial intelligence-based discontinuous reception for energy saving in 5G networks," *Electronics*, vol. 8, no. 7, p. 778, 2019.
- [57] R. E. Bellman and S. E. Dreyfus, *Applied dynamic programming*. Princeton university press, 2015.
- [58] N. C. Luong, D. T. Hoang, S. Gong, D. Niyato, P. Wang, Y.-C. Liang, and D. I. Kim, "Applications of deep reinforcement learning in communications and networking: A survey," *IEEE Communications Surveys & Tutorials*, vol. 21, no. 4, pp. 3133–3174, 2019.

- [59] Y.-H. Xu, X. Liu, W. Zhou, and G. Yu, "Generative Adversarial LSTM Networks Learning for Resource Allocation in UAV-served M2M Communications," *IEEE Wireless Communications Letters*, 2021.
- [60] Y. Fu and X. Wang, "Traffic Prediction-Enabled Energy-Efficient Dynamic Computing Resource Allocation in CRAN Based on Deep Learning," *IEEE Open Journal of the Communications Society*, vol. 3, pp. 159–175, 2022.
- [61] F. A. Gers, J. Schmidhuber, and F. Cummins, "Learning to forget: Continual prediction with LSTM," *Neural computation*, vol. 12, no. 10, pp. 2451–2471, 2000.
- [62] V. Eramo and T. Catena, "Application of an Innovative Convolutional/LSTM Neural Network for Computing Resource Allocation in NFV Network Architectures," *IEEE Transactions on Network and Service Management*, 2022.
- [63] Z. Chen, B. Wu, B. Li, and H. Ruan, "Expressway Exit Traffic Flow Prediction for ETC and MTC Charging System Based on Entry Traffic Flows and LSTM Model," *IEEE Access*, vol. 9, pp. 54 613–54 624, 2021.
- [64] M. Sharma, R. Pachori, and A. Rajendra, "Adam: a method for stochastic optimization," *Pattern Recogn. Lett.*, vol. 94, pp. 172–179, 2017.
- [65] *MATLAB version 9.7.0.1190202 (R2018b)*, The Mathworks, Inc., Natick, Massachusetts, 2018.



**David E. Ruiz-Guirola** received the B.Sc. (1st class honors, 2018) and M.Sc. (with distinction, 2019) degree in Telecommunications and Electronic Engineering from the Central University of Las Villas (UCLV), Santa Clara, Cuba. From 2018-2021 he served as an Associate Professor at UCLV. He joined the

Centre for Wireless Communications, University of Oulu, Finland, in 2021. He is currently pursuing the Ph.D. degree at the University of Oulu. His research interests include sustainable IoT, energy harvesting, wireless RF energy transfer, machine-type communications, machine learning, and traffic prediction.



**Carlos A. Rodríguez-López** received the B.Sc. and M.Sc. degrees in Electronic Equipment and Components and Telecommunications from the Central University of Las Villas (UCLV), Cuba, in 1990 and 2000, respectively. He is currently a Professor with the Department of Telecommunications, UCLV. His research

interests are in the area of wireless mobile communications, including visible light communications.



**Samuel Montejo-Sánchez** (IEEE M'17-SM'22) received the B.Sc., M.Sc., and D.Sc. degrees in telecommunications from the Central University of Las Villas (UCLV), Cuba, in 2003, 2007 and 2013, respectively. From 2003-2017, he was an Associate Professor at UCLV. Since 2018, he has been with the Programa Institucional de Fomento a la I+D+i (PIDi), Universidad Tecnológica Metropolitana

(UTEM). He leads the FONDECYT Iniciación No. 11200659 (Toward High Performance Wireless Connectivity for IoT and Beyond-5G Networks) project. His research interests include wireless communications, signal processing, sustainable IoT, and wireless RF energy transfer. He was a co-recipient of the 2016 Research Award from the Cuban Academy of Sciences.



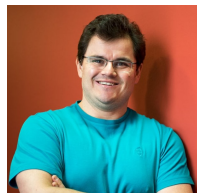
**Richard Demo Souza** (IEEE S'01-M'04-SM'12) received the D.Sc. degree in Electrical Engineering from the Federal University of Santa Catarina (UFSC), Brazil, in 2003. From 2004 to 2016 he was with the Federal University of Technology – Paraná (UTFPR), Brazil. Since 2017 he has been with UFSC, where he is a Professor. His research

interests are in the areas of wireless communications and signal processing. He has served as Editor or Associate Editor for the SBrT Journal of Communications and Information Systems, the IEEE Communications Letters, the IEEE Transactions on Vehicular Technology, the IEEE Transactions on Communications, and the IEEE IoT Journal. He is a co-recipient of the 2014 IEEE/IFIP Wireless Days Conference Best Paper Award, the supervisor of the awarded Best PhD Thesis in Electrical Engineering in Brazil in 2014, and a co-recipient of the 2016 Research Award from the Cuban Academy of Sciences.



**Onel L. A. López** (S'17-M'20) received the B.Sc. (1st class honors, 2013), M.Sc. (2017) and D.Sc. (with distinction, 2020) degree in Electrical Engineering from the Central University of Las Villas (Cuba), the Federal University of Paraná (Brazil), and the University of Oulu (Finland), respectively. He is a collaborator to the 2016 Research Award given by the Cuban

Academy of Sciences, a co-recipient of the 2019 IEEE EuCNC Best Student Paper Award, and the recipient of the 2020 best doctoral thesis award granted by Finland TEK and TFiF in 2021. He is co-author of the book entitled "Wireless RF Energy Transfer in the massive IoT era: towards sustainable zero-energy networks", Wiley, Dec 2021. He currently holds an Assistant Professorship (tenure track) in sustainable wireless communications engineering in the Centre for Wireless Communications (CWC), Oulu, Finland. His research interests include wireless communications, signal processing, sustainable IoT, and wireless RF energy transfer.



**Hirley Alves** (S'11-M'15) is Associate Professor and Head of the Machine-type Wireless Communications Group at the 6G Flagship, Centre for Wireless Communications, University of Oulu. He is actively working on massive connectivity and ultra-reliable low latency communications for future wireless networks, 5G

and 6G, full-duplex communications, and physical-layer security. In addition, he leads the URLLC activities for the 6G Flagship Program. He has received several awards and has been the organizer, chair, TPC, and tutorial lecturer for several renowned international conferences. He is the General Chair of the ISWCS'2019 and the General Co-Chair of the 1st 6G Summit, Levi 2019, and ISWCS 2021.